Publisher: GSA
Journal: GEOL: Geology
DOI:10.1130/G39398.1

Evidence for a dynamic grounding-line in outer Filchner Trough, Antarctica, until the early Holocene

Jan Erik Arndt[1], Claus-Dieter Hillenbrand[2], Hannes Grobe[1], Gerhard Kuhn[1], and Lukas Wacker[3]

[1]Alfred Wegener Institute Helmholtz Centre for Polar and Marine Research, Am Handelshafen 12, 27570 Bremerhaven, Germany

[2]British Antarctic Survey, High Cross Madingley Road, Cambridge, CB3 0ET, UK

[3]ETH Zürich, Laboratory of Ion Beam Physics, Schafmattstrasse 20, CH-8093 Zürich, Switzerland

ABSTRACT

Previous reconstructions of ice-sheet changes in Antarctica’s Weddell Sea sector since the Last Glacial Maximum (LGM) at 19–23 (calibrated) cal. kyr B.P. suffered from large uncertainties and were partly contradictory. As a consequence, the contribution of this sector to the LGM sea-level low stand and post-LGM sea-level rise was unclear. Furthermore, whether and how precursor water masses for Antarctic Bottom Water (AABW) were formed in the Weddell Sea Embayment under glacial conditions is unknown, as this today requires the existence of the floating Filchner-Ronne Ice Shelf. Here we present new marine geophysical and marine geological data from the outer shelf section of the Filchner paleo-ice stream trough documenting that grounded ice had advanced onto and retreated from the outer shelf prior to 27.5 cal. kyr B.P., i.e., more than 4,500 years before the LGM. The data reveal the presence of a stacked grounding-zone wedge (GZW) just south of 75°30′ S. This GZW was formed during two episodes of

grounding-line re-advance onto the outer shelf after 11.8 cal. kyr B.P., with data further inshore implying paleo-ice stream retreat from the GZW location prior to 8.7 cal. kyr B.P.. Our findings show that (i) ice-sheet build-up in the Weddell Sea sector made only limited contributions to the LGM sea-level low stand, (ii) ice-ocean interaction below an ice shelf in outer Filchner Trough could contribute to AABW production at the LGM, and (iii) numerical models need to take into account a highly dynamic ice-sheet behavior in regions of WAIS and EAIS confluence.

INTRODUCTION

Today, the West Antarctic Ice Sheet (WAIS) and the East Antarctic Ice Sheet (EAIS) drain ~20% of Antarctica's ice volume into the Weddell Sea Embayment (WSE; Figure 1 inset), where ~40% of AABW, a major component of the global ocean conveyor, are formed by ice-ocean interactions below and in front of the Filchner-Ronne Ice Shelf (Meredith, 2013). Despite its glaciological and oceanographic significance, however, the WSE is the Antarctic sector with the largest uncertainties in reconstructions of grounded ice-sheet extent at the LGM and the timing of post-LGM grounding-line retreat (RAISED Consortium, 2014). A review of geological data available from this sector presented two conflicting ice extent scenarios (Hillenbrand et al., 2014). For Filchner Trough, the largest cross-shelf trough in the WSE, the first scenario proposed a maximum grounding-line position on the inner shelf just south of 80 °S based on limited ice-sheet thickening reconstructed from terrestrial geomorphological data and cosmogenic nuclide surface exposure ages on erratics in the Shackleton Range (Fig. 1 inset, e.g., Hein et al., 2011). The second scenario, which is mainly based on geomorphological and sediment core data from the WSE shelf, concluded a grounding-

Publisher: GSA
Journal: GEOL: Geology
DOI:10.1130/G39398.1

line position at the shelf break, i.e., ~650 km further offshore. Recently, the feasibility of both LGM scenarios was confirmed by a flow-line modeling study (Whitehouse et al., 2017). Furthermore, cosmogenic-nuclide data from the Ellsworth Mountains (Fig. 1 inset) suggest that the LGM ice-sheet thickness was maintained at the WAIS into the early Holocene (Hein et al., 2016) and new glaciological evidence from ice rises has shown that ice-sheet retreat from the WSE shelf during the Middle and Late Holocene did not occur uniformly, but was characterized by switches in ice-stream flow and grounding-line re-advances (e.g., Winter et al., 2015; Kingslake et al., 2016).

Despite this recent research progress, it is still unclear whether the WSE contributed significantly to post LGM sea-level rise, including phases of rapid, global sea-level rise (meltwater pulses) (Golledge et al., 2014; Hein et al., 2016), and if and how AABW formed in the WSE under LGM conditions (Mackensen et al., 1996). Therefore, additional information from paleo-records is required. Here we present new swath bathymetry, acoustic sub-bottom profiler and sediment core data from the outer part of Filchner Trough (north of 75°50′ S) providing evidence that a highly dynamic ice-stream system existed there until the early Holocene.

MATERIALS

Most of the multibeam bathymetry data and acoustic sub-bottom profiles from the study area (Fig. 1a) were collected on expedition PS96 with RV “Polarstern” in austral summer 2015/2016 using the hull-mounted Atlas-Teledyne Hydrosweep DS3 and Parasound P-70 systems. Pre-existing bathymetric data were added to the new data set (GSA Data Repository[1]). Gravity cores PS96/079–3 and PS96/080–1 were recovered on

DOI:10.1130/G39398.1

cruise PS96 from the study area (Fig. 1a). Sampling and analytical procedures followed standard methods and are outlined in GSA Data Repository.

GLACIAL GEOMORPHOLOGY AND SUB-SEAFLOOR STRATIGRAPHY

Our new bathymetry data reveal a 15 km wide and ≥35 km long depression with a maximum depth of 745 m in the outer shelf section of Filchner Trough (Fig. 1a). The depression is bounded by a shallow (<700 m depth) western flank, while its eastern part is overlain by a ≤5 km wide and ~20 m high “terrace” (~720 m depth), which is bounded by a shallow eastern flank (<700 m depth). A wedge-shaped “sill” with a steep northern flank, a gentle backslope and a crest reaching a minimum depth of ~700 m is located to the south of the depression and the terrace. The seafloor within the depression and on the terrace is carved by highly elongated and parallel, NNE-directed lineations (up to 11 km length, 2–6 m amplitude, 200–400 m spacing), hereafter referred to as Lineations A and B, respectively (Fig. 1b). We interpret these lineations as mega-scale glacial lineations (MSGLs) formed at the base of fast flowing ice (cf. Clark, 1993; King et al., 2009; Stokes and Clark, 2001). The strike direction of both MSGL sets is nearly the same (A = ~15°, B = ~12°) and in common with the orientation of the central axis of Filchner Trough. On the backslope of the wedge-shaped sill and the shallow trough flanks, the seafloor is characterized by randomly oriented, slightly curved to curvilinear furrows (150 m to 500 m width, ~10 m average incision) that we interpret to have been eroded by iceberg keels into the seafloor under glacimarine conditions (e.g., Dowdeswell and Bamber, 2007; Klages et al., 2015). These iceberg ploughmarks occur down to a water depth of ~710 m around the depression. South of the sill they are observed down to ~730 m depth.

DOI:10.1130/G39398.1

The acoustic sub-bottom profiler data (Fig. 1b) show that in the depression a ~3 m thick horizontally stratified unit (acoustic facies AF1) drapes an acoustically transparent unit (AF2) of variable thickness (0–4 m). The surface of AF2 corresponds to Lineations A and its base is defined by a smooth and flat basal reflector. Draping AF1 continues underneath the wedge-shaped sill, which itself consists of a thick acoustic transparent unit (AF3). At the terrace, which also consists of AF3, AF1 splits into a thicker lower part dipping underneath the terrace and a thinner upper part, forming the near-seafloor sediments on the western slope of the terrace. On top of the terrace, where Lineations B are present, AF1 pinches out. Lineations A were formed on top of AF2, so this unit is interpreted to consist of soft deformation till that facilitated fast ice flow (cf. Alley et al., 1986; Ó Cofaigh et al., 2005). AF1 represents a drape of glacimarine sediments, whereas AF3 mainly corresponds to a soft deformation till, which is evident from the sediment cores (see below).

Based on the bathymetric findings and the sub-seafloor stratigraphy we interpret the wedge-shaped sill and the terrace as grounding-zone wedges (GZW, cf. Batchelor and Dowdeswell, 2015) and refer in the following to the terrace as GZW 1a and the wedge-shaped sill as GZW 1b. GZWs are formed at the grounding line of an ice stream by continuous till deposition during a period of grounding-line stillstand (Alley et al., 1989; Ó Cofaigh et al., 2008). The backslope of a newly formed GZW is typically characterized by MSGLs, such as Lineations B on GZW 1a, unless the maximum draft of icebergs after the grounding line has retreated further upstream is sufficient to obliterate the MSGL by ploughing, such as on GZW 1b (cf. Batchelor and Dowdeswell, 2015).

CORE LITHOLOGY AND CHRONOLOGY

Sediment core PS96/079–3 was retrieved from AF1 within the depression (Fig. 1a; GSA Data Repository). It recovered a 181 cm long sequence of predominantly terrigenous, laminated to stratified muds, sandy muds and muddy gravelly sands with relatively high water content (mean 32 wt.%), low shear strength (≤6.5 kPa) and variable wet-bulk density (mean 1.74 g cm^{-3}) and volume corrected magnetic susceptibility (Fig. 2a). The lithofacies of these sediments indicates deposition in a glacimarine setting, often under ice-shelf or permanent sea-ice cover (GSA Data Repository). The AMS ^{14}C date obtained from benthic foraminifera at 17 cm depth provided an age of 9934 ± 243 cal. yr B.P., while mixed benthic/planktic foraminifera from 150 cm depth gave an age of 27,530 ± 243 cal. yr B.P. (Fig. 2a; GSA Data Repository). The core show no indication of a glacial unconformity, subglacial over-compaction or till sedimentation and suggests deposition of normally consolidated glacimarine sediments since pre-LGM times.

Core PS96/080–1 was retrieved from Lineations B on GZW 1a (Fig. 1a) and recovered a 223 cm long sequence (Fig. 2b; GSA Data Repository). The upper 25 cm of the sediments consist of a massive muddy diamicton, which probably corresponds to the uppermost part of AF1 and bears some diatoms in the top 11 cm indicating the deposition of the near-surface sediments in a (seasonally) open marine setting (e.g., Domack et al., 1999). This unit is underlain by 26 cm of consolidated sandy mud with gravel- to pebble-sized intraclasts and a ≥172 cm thick purely terrigenous, homogenous muddy diamicton (GSA Data Repository). Within this lower diamicton, which corresponds to AF3 (Fig. 1b), water content is low (mean 21 wt.%), magnetic susceptibility and wet-bulk density are uniform, with the latter being relatively high (mean 1.98 g cm^{-3}), and shear strength increases down-core from ~5 to 16 kPa (Fig. 2b). The two AMS ^{14}C dates obtained from

Publisher: GSA
Journal: GEOL: Geology
DOI:10.1130/G39398.1

benthic foraminifera at 20 cm and 120 cm below surface provided ages of 15,436 ± 299 cal. yr B.P. and 11,836 ± 447 cal. yr B.P., respectively (Fig. 2b; GSA Data Repository). All the sedimentological properties of the lower muddy diamicton in core PS96/080–1 indicate its deposition as a soft deformation till at the base of an ice stream (GSA Data Repository). This interpretation is also consistent with the occurrence of Lineations B on top of the GZW 1a and the observed down-core age reversal suggesting subglacial reworking of foraminifer shells. In any case, the chronological constraints from core PS96/080–1 imply that GZWs 1a and 1b were deposited after 11.8 cal. kyr B.P..

HISTORY OF GROUNDING-LINE ADVANCE AND RETREAT

Our results allow us to constrain the advance and retreat of the Filchner paleo-ice stream during the Late Quaternary. During **phase 1**, i.e., at some time before 27.5 cal. kyr B.P., the ice stream had advanced seaward of the study area, thereby forming Lineations A. Anderson and Andrews (1999) linked the deposition of large amounts of ice-rafted debris on the Weddell Sea continental rise to a grounding-line position at the shelf break and reported its cessation, possibly coinciding with the end of phase 1, at ~29 cal. kyr B.P.. In **phase 2** the grounding line retreated south of the depression, probably between ~29 and 27.5 cal. kyr B.P., and allowed glacimarine deposition draping Lineations A to prevail in the study area throughout the LGM (Fig. 3a). The Filchner paleo-ice stream re-advanced during **phase 3**, i.e. after 11.8 cal. kyr B.P. and possibly during the onset of the Holocene at 11.7 cal. kyr B.P., thereby eroding previously deposited glacimarine sediments and reworking them. The grounding line stopped upstream of the depression but advanced further seaward along the eastern flank of Filchner Trough (Fig. 1a), thereby depositing the 20 m thick GZW 1a on top of Lineations A and the lower part of the stratified drape (Fig. 3b). The center of Filchner Trough was probably covered by an ice shelf during that time. In successive **phase 4,** the grounding line retreated upstream along the eastern flank of Filchner Trough but stopped just south of the depression or even re-advanced to this location, where it paused and deposited the 50 m thick GZW 1b across the center of the trough (Fig. 3c). Thereby, the toe of GZW 1b prograded over Lineations A and the stratified drape in the depression as well as over Lineations B on top of GZW 1a. Phase 4 took place before 8.7 cal. kyr B.P. when glacimarine conditions had established 220 km upstream in Filchner Trough (see date from core G7 in Hillenbrand et al., 2014, inset in Fig 1a, and GSA Data Repository). The chronological constraints (<3 k.y.) for the build-up of GZWs 1a and 1b (maximum thickness 50 m) imply subglacial depositional rates >1.7 cm yr^{-1}, confirming that GZW formation requires high rates of sediment delivery to a fast-flowing ice-stream margin (Batchelor and Dowdeswell, 2015). During **phase 5**, spanning the middle and late Holocene, the grounding line had retreated far upstream of our study area (e.g., Hillenbrand et al., 2014). Icebergs calved from the Filchner-Ronne Ice Shelf front eroded ploughmarks into GZW 1b and the shallow seafloor on the Filchner Trough flanks (Fig. 3d). While MSGLs on GZW 1b were obliterated by iceberg scouring, Lineations A and B that occur in deeper waters (>710 m depth) were protected from most iceberg keels by the surrounding shallower seafloor.

IMPLICATIONS AND CONCLUSIONS

Our data reveal that the Filchner paleo-ice stream had advanced onto the outermost WSE shelf north of 75°30′S and possibly to the shelf edge before, but not during the LGM, when the grounding line was located further landward, i.e., south of 75°40′S. Two re-advances onto the outer shelf (~75°30’S and ~75°40’S) occurred at the onset of the Holocene between 11.8 and 8.7 cal. kyr B.P.. These findings imply: (1) Ice in the WSE contributed little to meltwater pulses during the last deglaciation but was involved in Holocene sea-level rise, which is consistent with recent studies on LGM to Holocene ice-sheet thinning in the SW hinterland of the WSE (Hein et al., 2016). (2) AABW could be formed under an ice shelf that existed in outer Filchner Trough during the LGM, probably in conjunction with AABW production in glacial-time polynyas over the WSE slope (e.g., Mackensen et al., 1996) and under ice shelves covering the outer Ross Sea shelf (Anderson et al., 2014). (3) The Filchner paleo ice-stream grounding line underwent highly dynamical fluctuations on the outer WSE shelf until the early Holocene. These fluctuations probably are a response to major reorganizations of ice-stream flow resembling those reported from the inner shelf during the middle and late Holocene (e.g., Winter et al., 2015; Kingslake et al., 2016). Importantly, models suggest that only ice-flow reorganization re-directing the ice streams draining the WAIS into the Ronne Ice Shelf today (Foundation, Möller and Institute ice streams; Fig. 1) into Filchner Trough, would have enabled grounding-line advance to the outermost part of Filchner Trough (Whitehouse et al., 2017). Indeed, bathymetric evidence for such a paleo-flow pathway exists for Foundation Ice Stream (Larter et al., 2012), while glaciological findings show that the Möller and Institute ice streams fed into the Filchner paleo-ice stream until the Mid-Holocene (e.g., Winter et al., 2015). Ice flow switching and different histories of precipitation over the WAIS and EAIS possibly also explain the restricted LGM expansion and late (i.e. early Holocene) readvance of the Filchner paleo-ice stream. Pre-LGM advance and retreat of the EAIS could have blocked and delayed WAIS drainage through Filchner Trough until the early Holocene, which needs to be taken into account in ice-sheet models.

ACKNOWLEDGMENTS

We thank all captains, crews and scientists involved in collecting the data used in this study, especially Jean-Guy Nistad (AWI) and Boris Dorschel (AWI) for assistance on cruise PS96 and Michael Seebeck (AWI) and Maricel Williams (BAS) for laboratory support. We are grateful to Robert D. Larter (BAS) for providing the bathymetry data of cruise JR97. We thank John B. Anderson, Rob McKay and one anonymous reviewer for their comments that improved the work. J.E.A. was funded by the Deutsche Forschungsgemeinschaft (DFG, German Research Foundation) – AR 1087/1–1. This study is part of the Alfred Wegener Institute Helmholtz Centre for Polar and Marine Research program Polar Regions and Coasts in the changing Earth System (PACES II; J.E.A., H.G., G.K.) and the British Antarctic Survey's Polar Science for Planet Earth Programme (C.D.H.) which is funded by the Natural Environment Research Council (NERC).

REFERENCES CITED

Alley, R. B., Blankenship, D. D., Bentley, C. R., and Rooney, S. T., 1986, Deformation of till beneath ice stream B, West Antarctica, Nature, v. 322, p. 57-59, doi:10.1038/322057a0

Alley, R. B., Blankenship, D. D., Rooney, S. T., and Bentley, C. R., 1989, Sedimentation beneath ice shelves — the view from ice stream B, Marine Geology, v. 85, p.101-120, doi: 10.1016/0025-3227(89)90150-3.

Anderson, J.B., and Andrews, J.T., 1999, Radiocarbon constraints on ice sheet advance and retreat in the Weddell Sea, Antarctica: Geology, v. 27, p. 179–182, doi:10.1130/0091-7613(1999)027<0179:RCOISA>2.3.CO;2.

Anderson, J.B., et al., 2014, Ross Sea paleo-ice sheet drainage and deglacial history during and since the LGM: Quaternary Science Reviews, v. 100, p. 31–54, doi:10.1016/j.quascirev.2013.08.020.

Batchelor, C.L., and Dowdeswell, J.A., 2015, Ice-sheet grounding-zone wedges (GZWs) on high-latitude continental margins: Marine Geology, v. 363, p. 65–92, doi:10.1016/j.margeo.2015.02.001.

Clark, C.D., 1993, Mega-scale glacial lineations and cross-cutting ice-flow landforms: Earth Surface Processes and Landforms, v. 18, p. 1–29, doi:10.1002/esp.3290180102.

Domack, E.W., Jacobson, E.A., Shipp, S., and Anderson, J.B., 1999, Late Pleistocene-Holocene retreat of the West Antarctic Ice-Sheet system in the Ross Sea: Part 2 - Sedimentologic and stratigraphic signature: Geological Society of America Bulletin, v. 111, p. 1517–1536, doi:10.1130/0016-7606(1999)111<1517:LPHROT>2.3.CO;2.

Dowdeswell, J.A., and Bamber, J.L., 2007, Keel depths of modern Antarctic icebergs and implications for sea-floor scouring in the geological record: Marine Geology, v. 243, p. 120–131, doi:10.1016/j.margeo.2007.04.008.

Golledge, N.R., Menviel, L., Carter, L., Fogwill, C.J., England, M.H., Cortese, G., and Levy, R.H., 2014, Antarctic contribution to meltwater pulse 1A from reduced Southern Ocean overturning: Nature Communications, v. 5, p. 5107, doi:10.1038/ncomms6107.

Hein, A.S., Fogwill, C.J., Sugden, D.E., and Xu, S., 2011, Glacial/interglacial ice-stream stability in the Weddell Sea embayment, Antarctica: Earth and Planetary Science Letters, v. 307, p. 211–221, doi: 10.1016/j.epsl.2011.04.037.

Hein, A.S., Marrero, S.M., Woodward, J., Dunning, S.A., Winter, K., Westoby, M.J., Freeman, S.P.H.T., Shanks, R.P., and Sugden, D.E., 2016, Mid-Holocene pulse of thinning in the Weddell Sea sector of the West Antarctic ice sheet: Nature Communications, v. 7, p. 12511, doi:10.1038/ncomms12511.

Hillenbrand, C.-D., et al., 2014, Reconstruction of changes in the Weddell Sea sector of the Antarctic Ice Sheet since the Last Glacial Maximum: Quaternary Science Reviews, v. 100, p. 111–136, doi:10.1016/j.quascirev.2013.07.020.

King, E.C., Hindmarsh, R.C.A., and Stokes, C.R., 2009, Formation of mega-scale glacial lineations observed beneath a West Antarctic ice stream: Nature Geoscience, v. 2, p. 585–588, doi:10.1038/ngeo581.

Kingslake, J., Martín, C., Arthern, R.J., Corr, H.F.J., and King, E.C., 2016, Ice-flow reorganization in West Antarctica 2.5 kyr ago dated using radar-derived englacial flow velocities: Geophysical Research Letters, v. 43, p. 9103–9112, doi:10.1002/2016GL070278.

Klages, J. P., Kuhn, G., Graham, A. G. C., Hillenbrand, C. D., Smith, J. A., Nitsche, F. O., Larter, R. D., and Gohl, K., 2015, Palaeo-ice stream pathways and retreat style in the easternmost Amundsen Sea Embayment, West Antarctica, revealed by combined multibeam bathymetric and seismic data: Geomorphology, v. 245, p. 207-222, doi: 10.1016/j.geomorph.2015.05.020.

Larter, R.D., Graham, A.G.C., Hillenbrand, C.-D., Smith, J.A., and Gales, J.A., 2012, Late Quaternary grounded ice extent in the Filchner Trough, Weddell Sea, Antarctica: New marine geophysical evidence: Quaternary Science Reviews, v. 53, p. 111–122, doi:10.1016/j.quascirev.2012.08.006.

Mackensen, A., Hubberten, H.-W., Scheele, N., and Schlitzer, R., 1996, Decoupling of õ$^{13}\Sigma CO_2$ and phosphate in recent Weddell Sea deep and bottom water: Implications for glacial Southern Ocean paleoceanography: Paleoceanography, v. 11, p. 203–215, doi:10.1029/95PA03840.

Meredith, M.P., 2013, Oceanography: Replenishing the abyss: Nature Geoscience, v. 6, p. 166–167, doi:10.1038/ngeo1743.

Ó Cofaigh, C., Dowdeswell, J. A., Allen, C. S., Hiemstra, J. F., Pudsey, C. J., Evans, J., and Evans, D.J.A., 2005, Flow dynamics and till genesis associated with a marine-based Antarctic palaeo-ice stream: Quaternary Science Reviews, v. 24, p. 709–740, doi:10.1016/j.quascirev.2004.10.006.

Ó Cofaigh, C., Dowdeswell, J. A., Evans, J., and Larter, R. D., 2008, Geological constraints on Antarctic palaeo-ice-stream retreat, Earth Surface Processes and Landforms, v. 33, p. 513-525, doi:10.1002/esp.1669

Reconstruction of Antarctic Ice Sheet Deglaciation (RAISED) Consortium, 2014, A community-based geological reconstruction of Antarctic Ice Sheet deglaciation since the Last Glacial Maximum: Quaternary Science Reviews, v. 100, p. 1–9, doi:10.1016/j.quascirev.2014.06.025.

Stokes, C.R., and Clark, C.D., 2001, Palaeo-ice streams, Quaternary Science Reviews, v. 20, p. 1437-1457, doi:10.1016/S0277-3791(01)00003-8.

Whitehouse, P.L., Bentley, M.J., Vieli, A., Jamieson, S.S.R., Hein, A.S., and Sugden, D.E., 2017, Controls on Last Glacial Maximum ice extent in the Weddell Sea embayment, Antarctica: Journal of Geophysical Research, Earth Surface, v. 122, p. 371–397, doi:10.1002/2016JF004121.

Winter, K., Woodward, J., Ross, N., Dunning, S. A., Bingham, R. G., Corr, H. F. J., and Siegert, M. J., 2015, Airborne radar evidence for tributary flow switching in Institute Ice Stream, West Antarctica: Implications for ice sheet configuration and dynamics: Journal of Geophysical Research Earth Surface, v. 120, p. 1611–1625.

FIGURE CAPTIONS

Figure 1. A: Bathymetry of the study area in outer Filchner Trough showing a depression (blue to yellow) with grounding zone wedge (GZW) 1a on its eastern side (yellow) and GZW 1b (orange/red) to the south. Note NNE striking mega-scale lineations within the depression (Lineations A) and on GZW 1a (Lineations B) and iceberg ploughmarks on top of GZW 1b and the trough flanks. White circles mark sites of studied cores. Inset shows the location of the study area (red box) within the wider Antarctic context and location of core G7; EAIS = East Antarctic Ice Sheet, WAIS = West Antarctic Ice Sheet, FRIS = Filchner Ronne Shelf Ice, FT = Filchner Trough, WSE = Weddell Sea Embayment, EM = Ellsworth Mountains, SR = Shackleton Range, I = Institute Ice Stream, M = Möller Ice Stream, F = Foundation Ice Stream. B: Acoustic sub-bottom profile across the depression (with Lineations A), GZW 1a (with Lineations B), and GZW 1b (for location see A); stratified acoustic facies (AF1) and transparent acoustic

facies (AF2 and AF3) are also indicated. Note the splitting of AF1 at GZW 1a into a top layer draping the toe of GZW 1a and a bottom layer dipping under GZW 1a and the continuation of AF1 underneath GZW 1b.

Figure 2. Lithofacies, shear strength, wet-bulk density (WBD), magnetic susceptibility, water content, grain-size composition of the sediment matrix and AMS ^{14}C dates for cores PS96/079–3 (A) and PS96/080–1 (B).Lithofacies: Ml: laminated mud, MGSl: laminated and stratified mud alternating with gravelly sandy mud and gravelly muddy sand, Mf: folded mud, MSI: consolidated sandy mud with gravel- to pebble-sized intraclasts, SGMm: massive gravelly muddy sand with inclined (erosional) base, Dmb: massive muddy diamicton with some diatoms, Dmt:
massive, purely terrigenous muddy diamicton (for details, see GSA Data Repository).

Figure 3. Cartoon of environmental conditions during different phases of the last glacial cycle in the study area (for details see text). A: Phase 2: glacimarine conditions with possible ice-shelf cover lead to sediment draping (gray) of Lineations A (yellow) which were formed during Phase 1 (not shown). B: Phase 3: after its advance to outer Filchner Trough a stillstand of the grounding-line causes the formation of GZW 1a with Lineations B at the eastern trough edge and in the trough center south of the depression. C: Phase 4: after a short retreat the grounding-line re-advances in the trough center and its subsequent stillstand causes the formation of GZW 1b with Lineations B on its top. D: Phase 5: under marine conditions icebergs float through the study area and erode ploughmarks into the trough flanks and the top of GZW 1b.

Publisher: GSA
Journal: GEOL: Geology
DOI:10.1130/G39398.1

[1]GSA Data Repository item 2017xxx, xxxxxxxx, is available online at http://www.geosociety.org/datarepository/2017/ or on request from editing@geosociety.org.

Figure 1 Click here to download Figure Figure_1_revision.tif

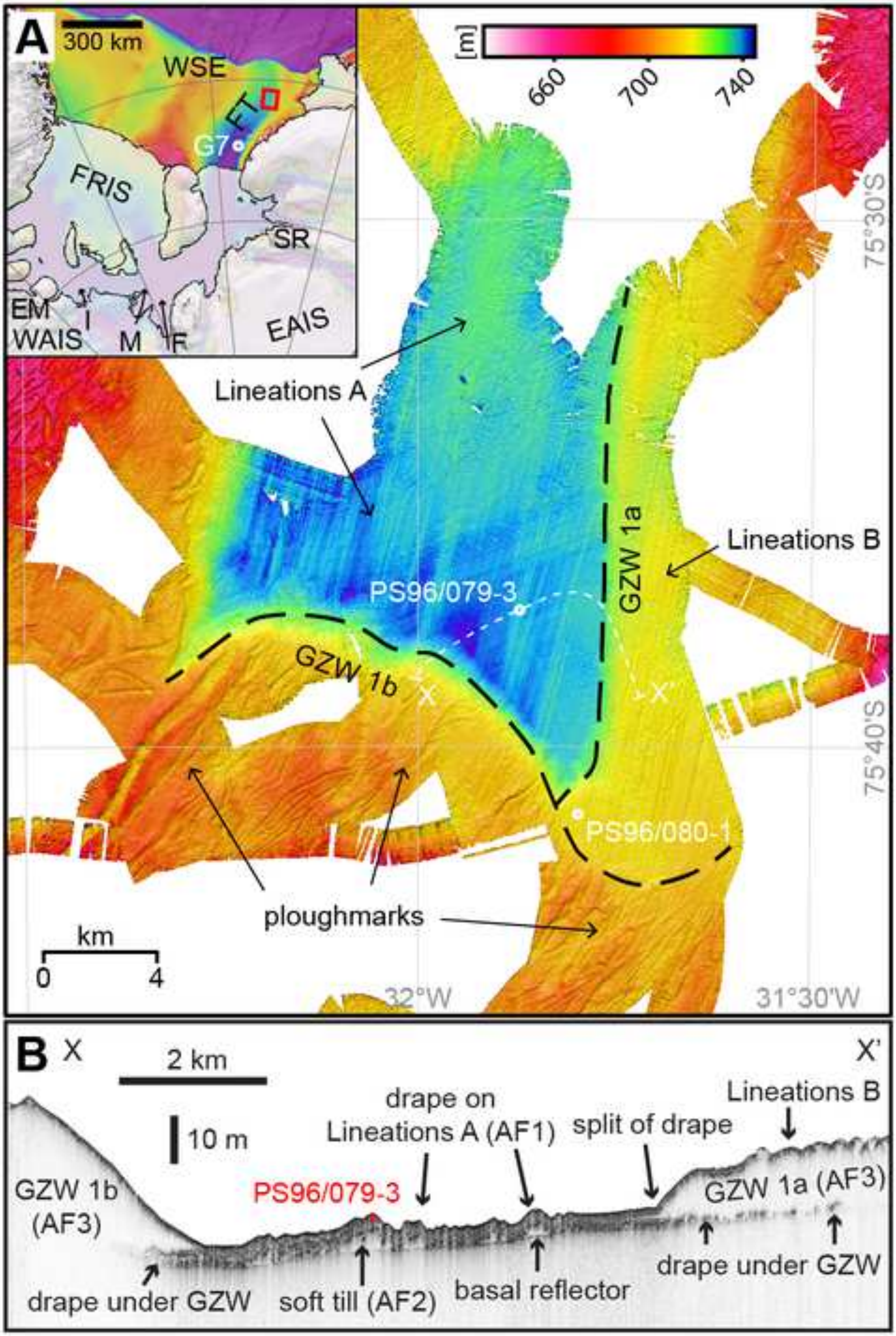

Figure 2

Click here to download Figure Fig2rev.tif

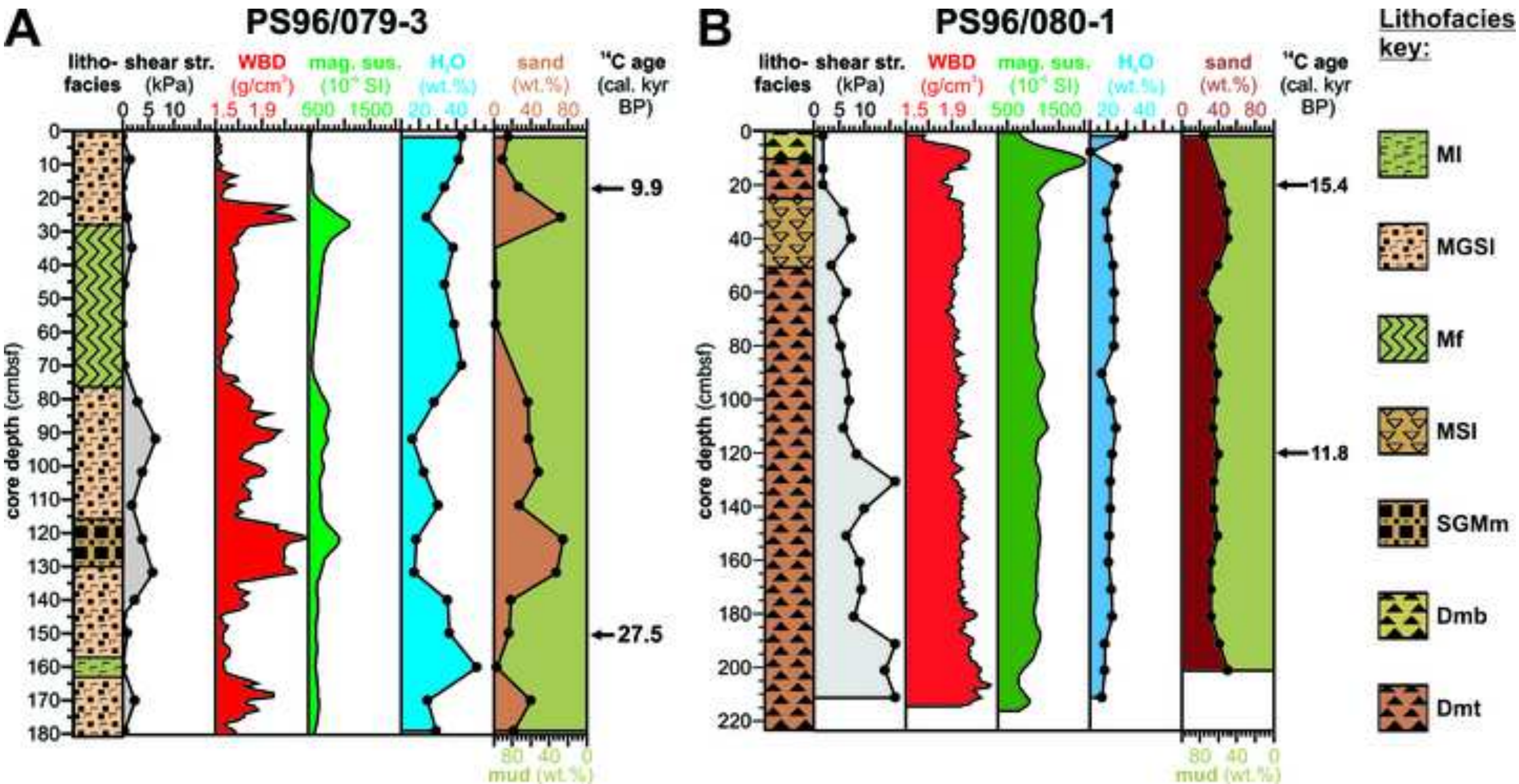

Figure3

Click here to download Figure Figure_3_Phases-01.tif

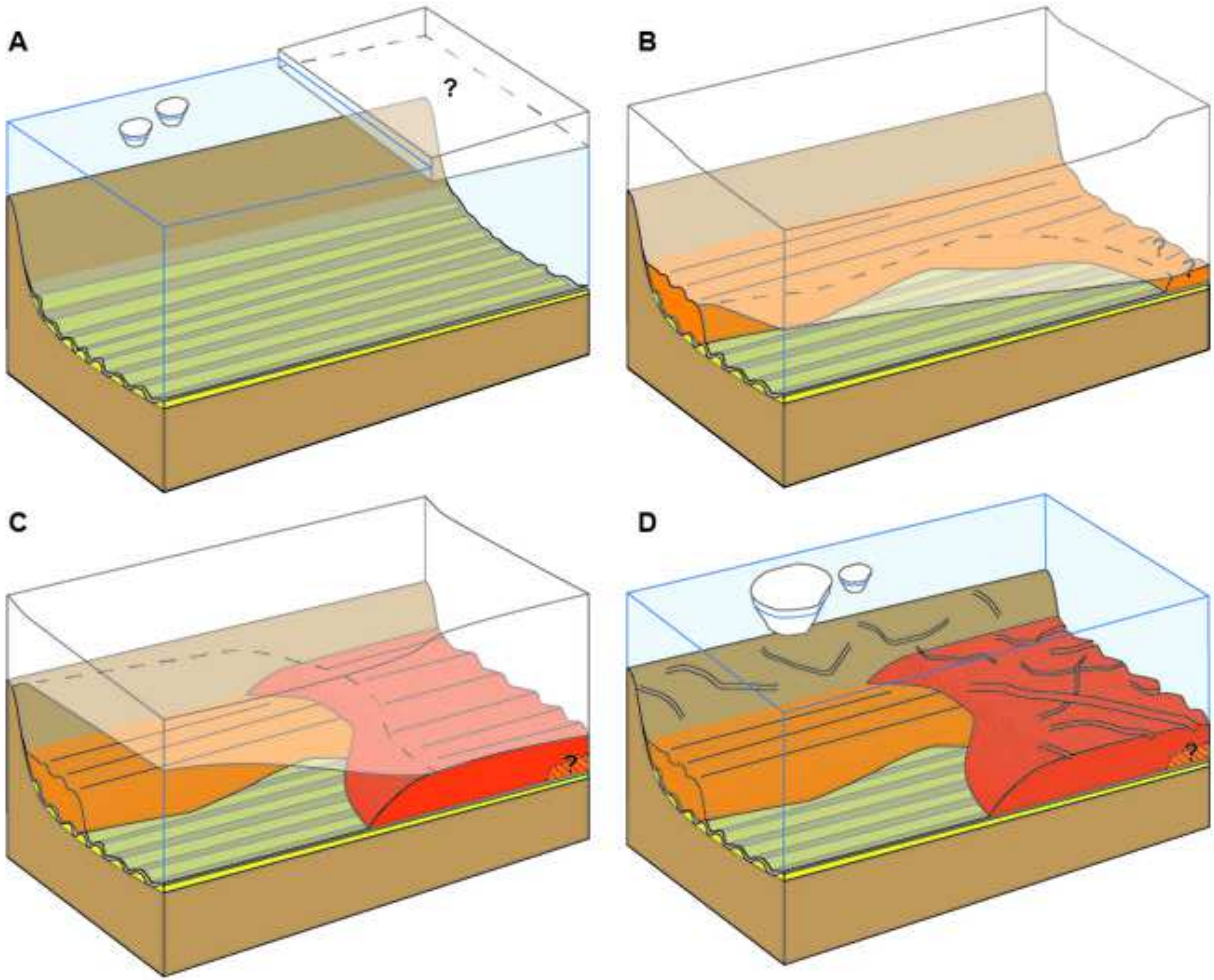

GSA Data Repository [# will be assigned after acceptance]

Evidence for a dynamic grounding-line in outer Filchner Trough, Antarctica, until the early Holocene

Jan Erik Arndt, Claus-Dieter Hillenbrand, Hannes Grobe, Gerhard Kuhn, and Lukas Wacker

MATERIAL, METHODS AND LABORATORY TECHNIQUES

Marine geophysical data

Most of the multibeam bathymetry data and acoustic sub-bottom profiles from the study area (Fig. 1a) were collected on expedition PS96 with RV *Polarstern* in austral summer 2015/2016 using the hull-mounted Atlas-Teledyne Hydrosweep DS3 and Parasound P-70 systems (Schröder, 2016). Pre-existing bathymetric data acquired during expeditions JR97 (2005) with RRS *James Clark Ross* using a Kongsberg-Simrad EM120 system and ANT-VIII/5 (1989/1990) with RV *Polarstern* using an Atlas Hydrosweep DS1 system (Miller and Oerter, 1991) were added to the bathymetry map of the study area. All bathymetric data were corrected on board by applying sound velocity profiles derived from conductivity-temperature-depth casts and post-processed to reject outlying soundings in CARIS Hips & Sips or in MB System, respectively. The final database was jointly gridded at 25 × 25 m resolution with a weighted moving average gridding algorithm in QPS Fledermaus.

Marine geological data

Methods: Gravity cores PS96/079-3 and PS96/080-1 were recovered on cruise PS96 from the study area (Fig. 1a; Table DR1) (Schröder, 2016). Physical properties (magnetic susceptibility, wet bulk density and P-wave velocity) were measured at 1-cm intervals on the whole cores with a GEOTEK multi-sensor core logger (MSCL) at the Alfred Wegener Institute in Bremerhaven. The cores were then split into working and archive halves, and their lithology and sedimentary structures were described visually, using X-radiographs and using smear slides. Shear strength was measured on the working halves of the cores with a hand-held shear vane. Water content and grain-size composition were analyzed on discrete samples taken from the cores. Water content was determined by weighing of the wet and freeze-dried samples, and gravel (>2 mm), sand (63 µm-2 mm) and mud (2 µm-63 µm) contents were analyzed by wet and dry sieving of 1-cm thick sediment samples taken from the working halves of the cores (volume: ca. 50 cm^3). Because gravel content may not be determined in a statistically reliable way on samples of this volume, we only present the sand and mud contents in Figure 2, which inform on the grain-size composition of the matrix of the sediments. Gravel and pebble abundance was evaluated visually and on the X-radiographs. The sand fraction was investigated under a microscope for the presence of calcareous microfossils.

Lithofacies classification and interpretation: The sediments recovered in cores PS96/079-3 and PS96/080-1 were assigned to seven different lithofacies, with each facies occurring in one of the cores only. The characteristics of each lithofacies and the interpretation of their depositional and their paleoenvironmental settings, which followed previously published literature on lithofacies in marine sediment cores from glaciated continental margins, are given in Table DR1. X-radiograph examples for each lithofacies are given in Figure DR**5**.

Chronology: Two horizons in each core were identified, which contained a few calcareous foraminifer shells (benthic species *Globocassidualina* spp. and *Cibicidoides* spp. and planktic species *Neogloboquadrina pachyderma* sinistral). Importantly, the two dated horizons in core PS96/079-3 are from lithofacies showing no indication of sediment reworking by gravitational downslope or glacial processes (Fig. DR6). All the foraminifer shells were picked for MICADAS AMS ^{14}C dating (Wacker et al., 2010) at the Laboratory of Ion Beam Physics, ETH Zürich. The ^{14}C dates were calibrated with the CALIB 7.1 calibration program (Stuiver and Reimer, 1993) using a regional marine reservoir correction of 1215±30 years (Hillenbrand et al., 2012) and the MARINE13 calibration dataset (Reimer et al., 2013) (Table DR2). For the full set of core photos and X-radiographs of cores PS96/079-3 and PS96/080-1, see https://doi.org/10.1594/PANGAEA.864391 and https://doi.org/10.1594/PANGAEA.864392, respectively.

Table DR1: Summary of lithofacies observed in the studied cores, and inferred processes and paleoenvironments. Preferred interpretations for each lithofacies are underlined. References: 1) McKay et al., 2009; 2) McKay et al., 2012; 3) Passchier et al., 2011; 4) Tripsanas et al., 2008; 5) Hillenbrand et al., 2010; 6) Licht et al., 1999; 7) Domack et al., 1999.

Facies	Core	Depth (cmbsf)	Lithology and sedimentary structure	Depositional process and environmental setting
Ml	PS96/079-3	[156/158]-[162/164]	laminated mud	Hemipelagic suspension settling[1,2]
MGSl	PS96/079-3	0-28 76-117 [129/132]-[156/158] [162/164]-181.5	laminated and stratified mud alternating with gravelly sandy mud and gravelly muddy sand	Suspension settling from turbid plumes[1,3], current-influenced glacimarine deposition[3], hemipelagic sedimentation with deposition of ice-rafted debris (IRD)[1,3]
Mf	PS96/079-3	28-76	folded mud	Debris flow[4], slump[4]
SGMm	PS96/079-3	117-[129/132]	massive gravelly muddy sand with inclined (erosional) base	Redeposition by mass flow[1,3], ice-shelf collapse sediment[3]
MSI	PS96/080-1	25-51	consolidated sandy mud with gravel- to pebble-sized intraclasts	Glacimarine deposition proximal to grounding line[2], mass flow deposit[2]
Dmb	PS96/080-1	0-[10/11]	massive muddy diamicton with some microfossils (here: diatoms)	Glacimarine deposition proximal to grounding line[5,6], iceberg-rafted diamicton[5,7], iceberg turbate[5,6]
Dmt	PS96/080-1	[10/11]-25 51-223	massive, purely terrigenous muddy diamicton	Subglacial till deposition[1-3,5-7], IRD rainout proximal to grounding line[1-3], glacigenic debris flow[1,5]

Table DR2: Locations, conventional and calibrated AMS ^{14}C dates on calcareous microfossils from the investigated and previously published sediment cores from the Weddell Sea (for uncertainties affecting ^{14}C dating of Antarctic shelf sediments, see Heroy and Anderson, 2007). Sample depths are given in centimetres below seafloor (cmbsf). All ^{14}C-dates were corrected using an offset (ΔR) of 815±30 years from the global marine reservoir effect (R) of 400 years in accordance with both an uncorrected ^{14}C-date of seafloor surface sediments from the uppermost continental slope (see conventional ^{14}C-age given in italics) and previous studies from around Antarctica (e.g. RAISED Consortium, 2014). The corrected ^{14}C-dates were calibrated with the CALIB Radiocarbon Calibration Program version 7.1.0html (http://calib.qub.ac.uk/calib/; Stuiver and Reimer, 1993) using the MARINE13 calibration dataset (Reimer et al., 2013). Errors of calibrated dates are given as a 2σ range. The ^{14}C-dates marking minimum ages for grounded ice retreat from a core site are highlighted in bold. Coring devices: GBC: giant box core, GC: gravity core, PH: phleger core, PC: piston core. Dated calcareous microfossils comprise benthic foraminifera (bF: unspecified benthic foraminifera, C: *Cibicides* spp., G: *Globocassidulina* spp.), planktic foraminifera (N: *Neogloboquadrina pachyderma* sinistral) and bryozoans (B). If known, number of dated foraminifer shells is also given. X-radiographs of dated horizons in cores PS96/079-3 and PS96/080-1 are shown in Figure DR6. Preservation of all dated foraminifer shells was modest. References: A) Hillenbrand et al., 2012; B) Stolldorf et al., 2012; C) Anderson and Andrews, 1999.

Area	Cruise	Gear	Core ID	Latitude (°)	Longitude (°)	Water depth (m)	Core recovery (m)	Sample depth (cmbsf)	Laboratory code	Dated microfossils (n)	Conventional ^{14}C age ±error (yrs BP)	R (yrs)	ΔR ±error (yrs)	Calibrated ^{14}C age ±error (cal yrs BP)	Reference
Filchner Trough (outer shelf)	PS96	GC	PS96/79-3	-75.6250	-31.8722	763	1.81	17	ETH-74959.1.1	G (35), C (1)	9995±75	400	815±30	9934±243	this study
								150	ETH-74960.1.1	G (4), C (1), N (3)	**24560±250**	**400**	**815±30**	**27530±387**	this study
Filchner Trough (outer shelf)	PS96	GC	PS96/80-1	-75.6890	-31.7983	720	2.23	20	ETH-74961.1.1	G (28)	14120±90	400	815±30	15436±299	this study
								120	ETH-74962.1.1	G (21)	11415±85	400	815±30	11836±447	this study
E' Crary Fan (uppermost slope)	ANT-IV/3	GBC	PS1418-1	-74.4750	-35.5933	769	4.89	0-1	HD-13273	B	*1215±30*	*N/A*	*N/A*	*[0]*	ref. A
Filchner Trough (mid-shelf)	IWSOE69	PC	G7	-77.3330	-36.5500	1079	1.57	0-5	CCAMS-95867	bF	**9040±100**	400	815±30	**8738±273**	ref. B
Weddell Sea (continental rise)	IWSOE68	PH	37	-69.6833	-46.2670	3777	0.90	56-60	AA-24841	N	26570±490	400	815±30	29580±1092	ref. C
Weddell Sea (continental rise)	IWSOE68	PH	52	-67.3667	-47.3667	3768	0.85	42-47	AA-19910	N (800)	25900±620	400	815±30	28930±1287	ref. C

Figure DR1: Locations of the investigated and previously published sediment cores from the Weddell Sea. Background data from IBCSO V1.0, Arndt et al. 2013.

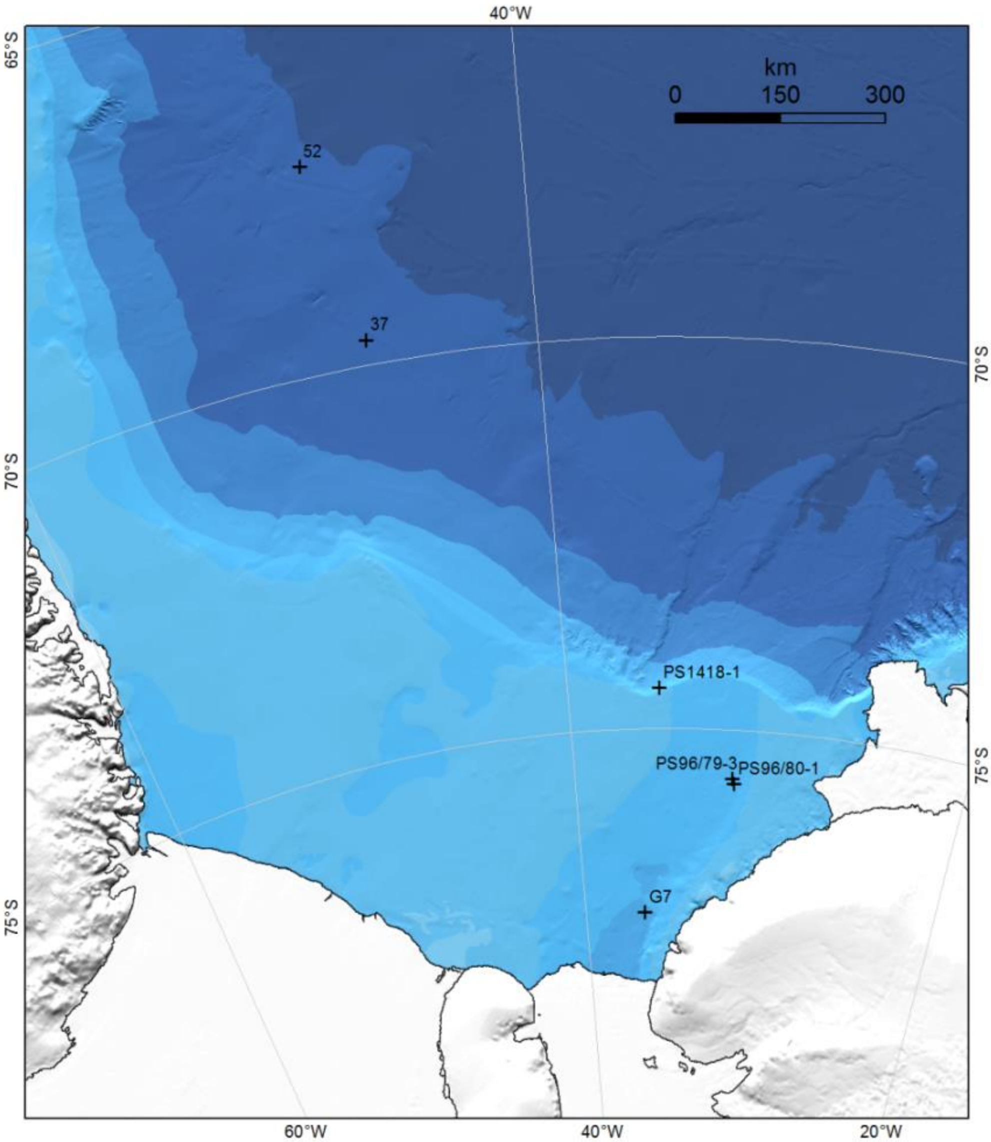

Figure DR2: (A) Line drawing of interpreted submarine landforms with locations of bathymetric profiles: (B) along the trough centre over GZW 1b; (C) across GZW 1a and GZW 1b.

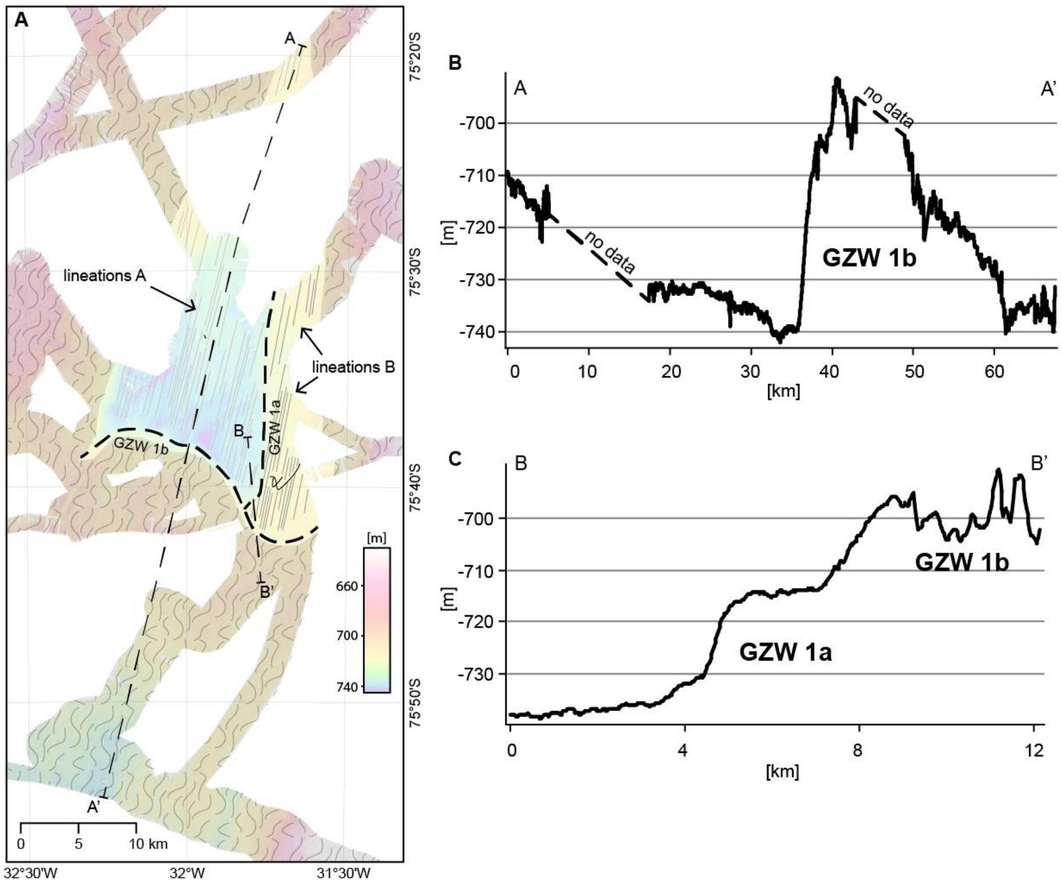

Figure DR3: Detailed sub-bottom profiler (PARASOUND) transects from core locations and other transitions from draped lineations to GZW 1a and 1b.

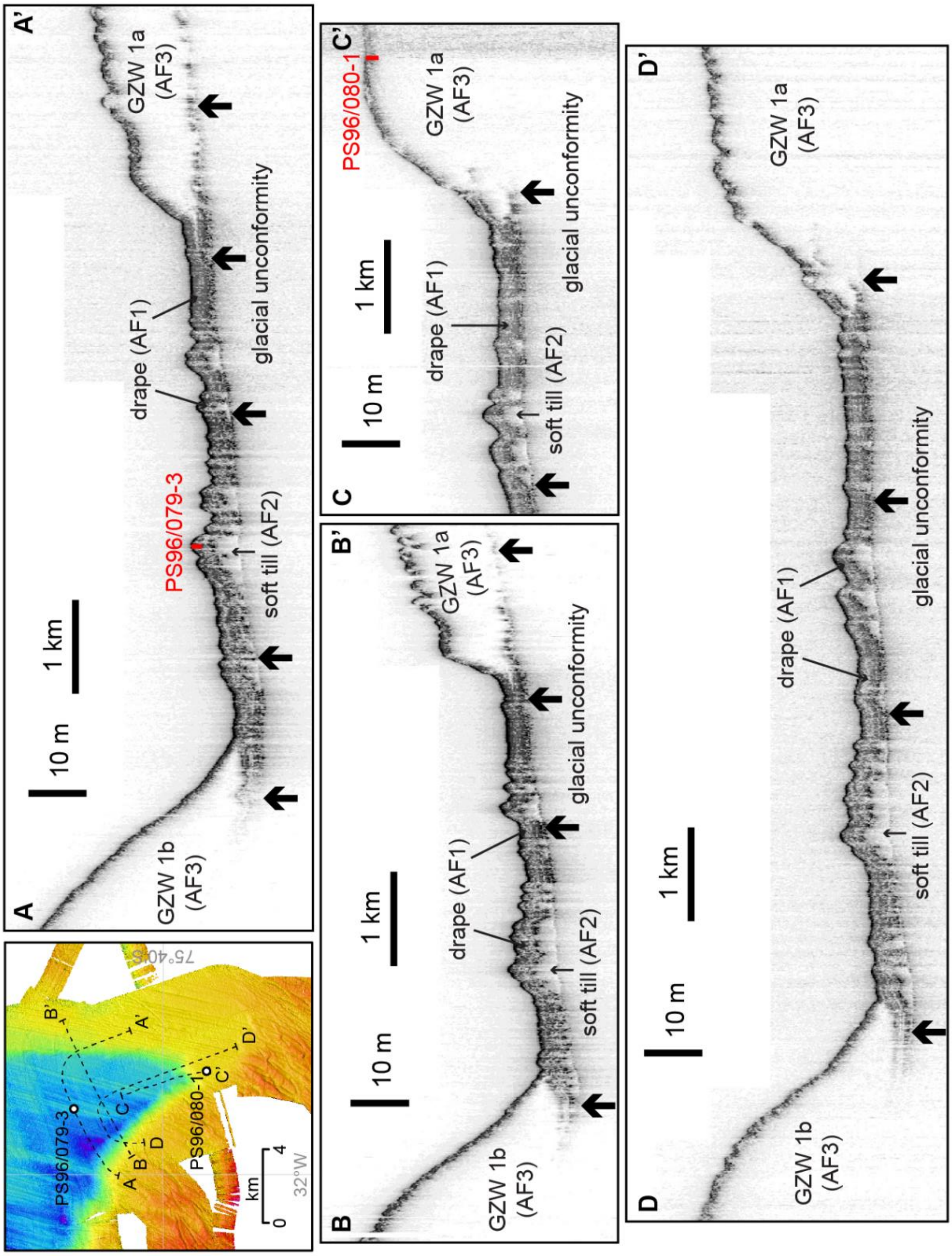

Figure DR4: Detailed bathymetric maps of core locations PS96/079-3 and PS96/080-1.

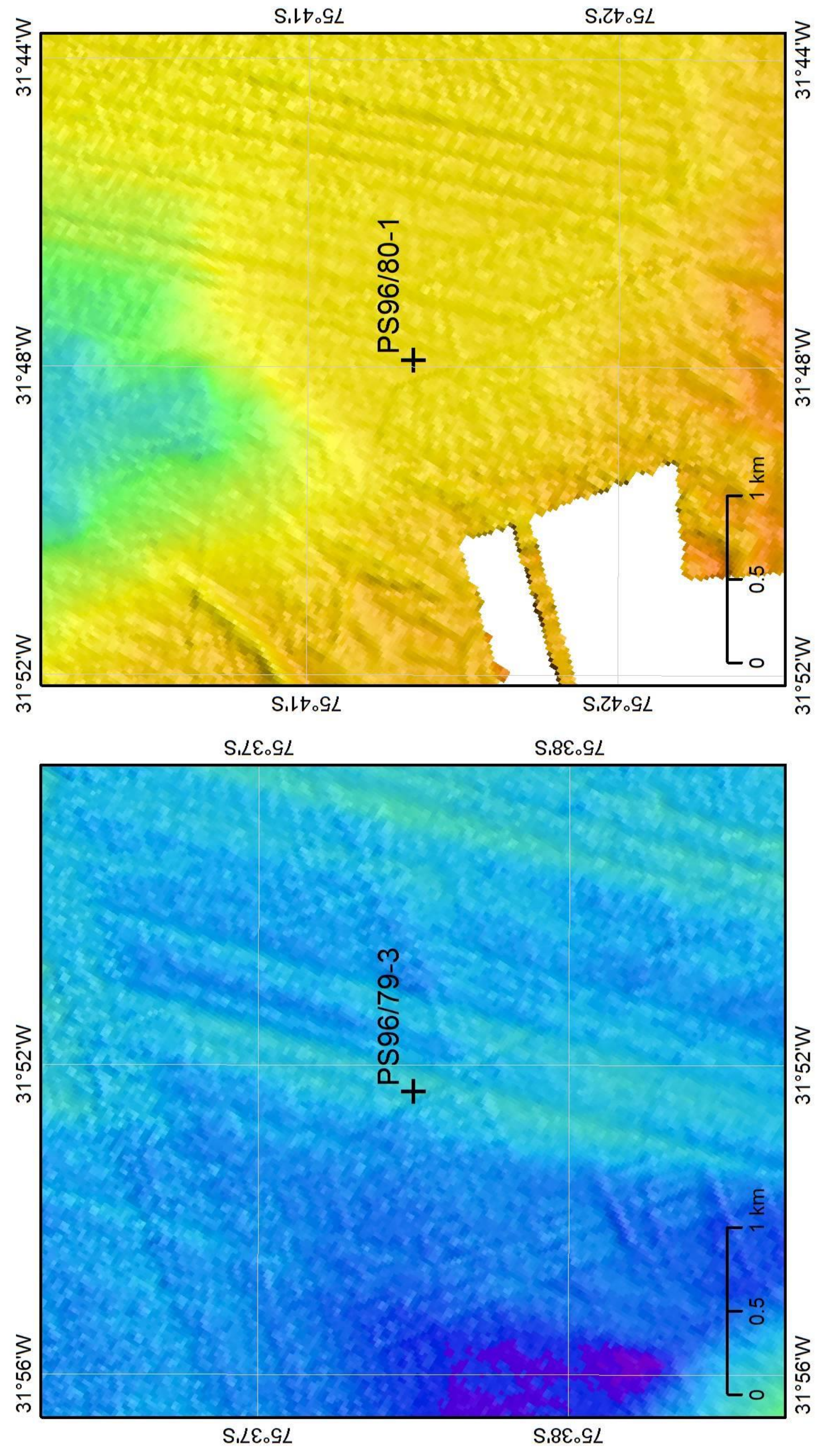

Figure DR5 (next 3 pages): X-radiograph (positives) examples for lithofacies identified in the studied cores. PS96/079-3: a) Laminated mud (Ml) in between laminated and stratified mud alternating with gravelly sandy mud and gravelly muddy sand (MGSl); b) laminated and stratified mud alternating with gravelly sandy mud and gravelly muddy sand (MGSl); c) folded mud (Mf); d) massive gravelly muddy sand with inclined, erosional base (SGMm) on top of laminated and stratified mud alternating with gravelly sandy mud and gravelly muddy sand (MGSl). PS96/080-1: e) consolidated sandy mud with gravel- to pebble-sized intraclasts (MSI); f) massive muddy diamicton with some diatoms (Dmb) on top of massive, purely terrigenous muddy diamicton (Dmt); g) massive, purely terrigenous muddy diamicton (Dmt). Each X-radiograph is 10 cm wide, and white areas are voids in the sediment slabs caused by large gravel grains/pebbles or sample processing.

Figure DR5 (continued)

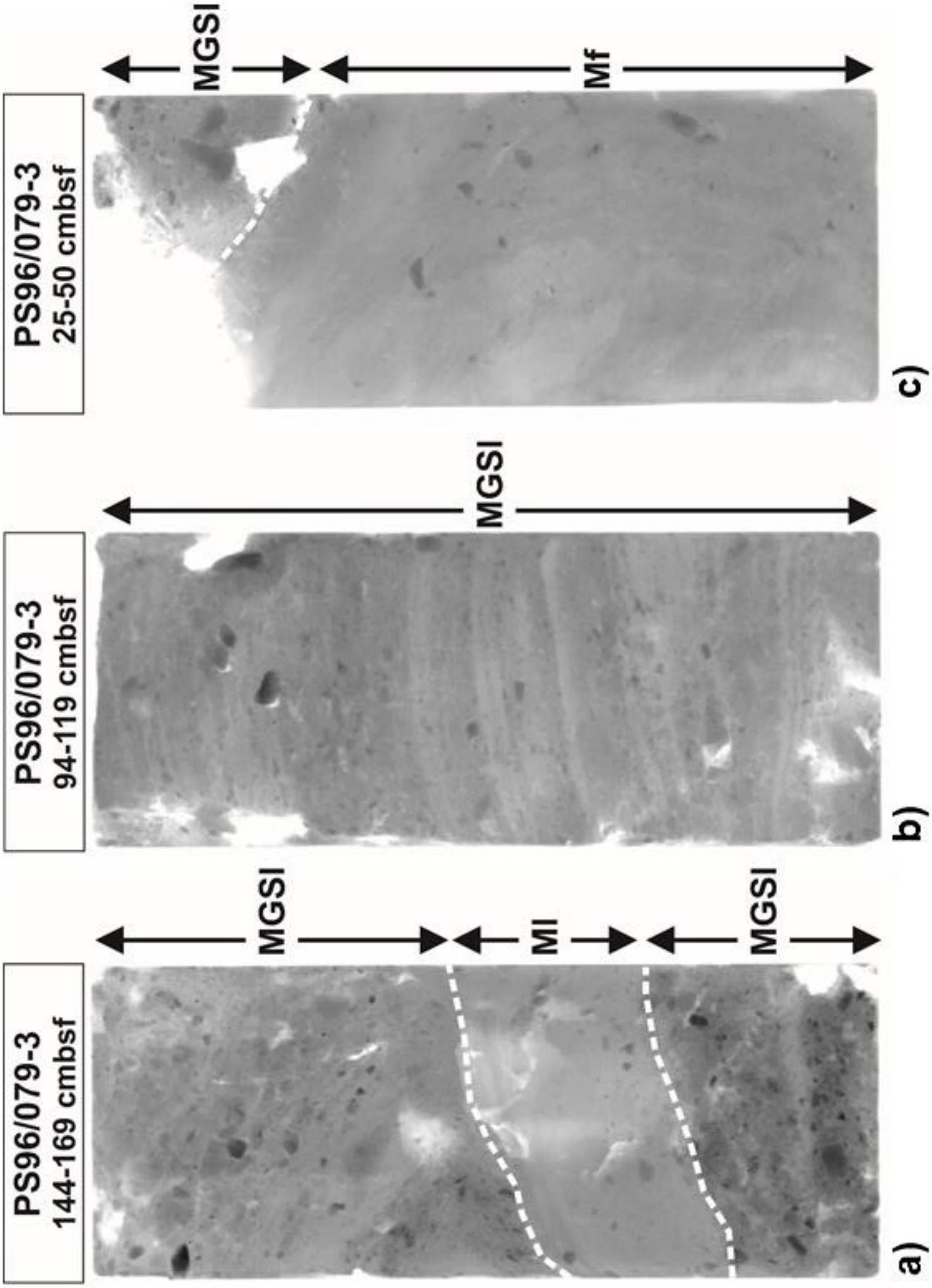

Figure DR5 (continued)

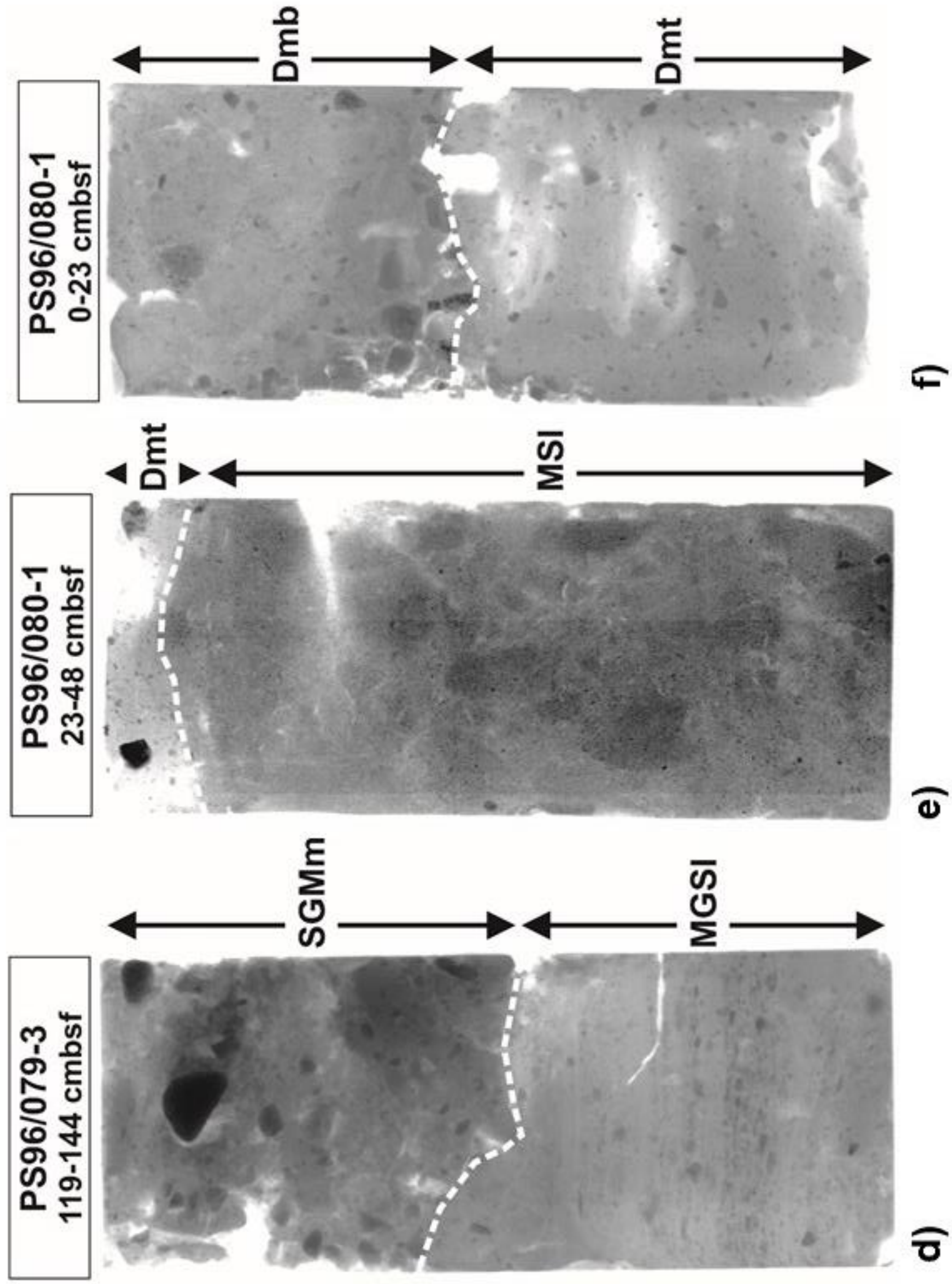

Figure DR5 (continued)

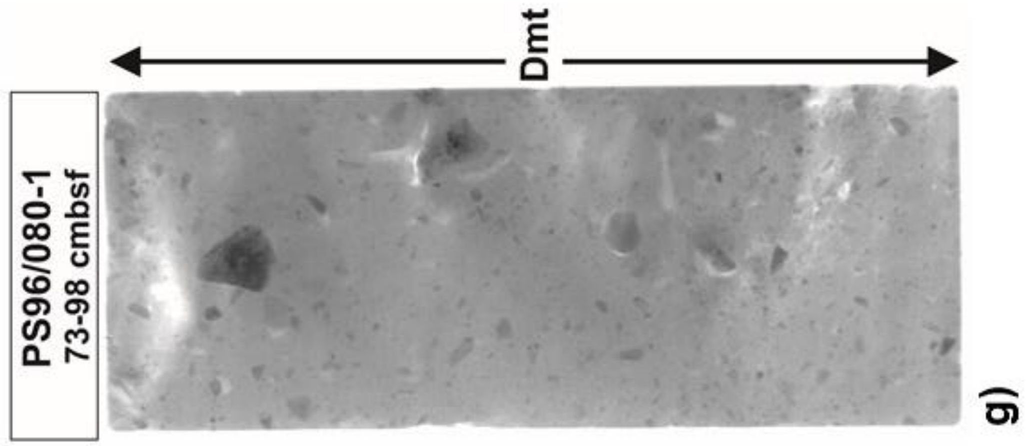

Figure DR6 (next page): Sample horizons of AMS ^{14}C dated foraminifer shells in cores PS96/079-3 and PS96/080-1 (orange boxes) in relation to sediment lithology visualised by X-radiograph positives. a) PS96/079-3 17 cmbsf (cm below surface): b) PS96/079-3 150 cmbsf: c) PS96/080-1 20 cmbsf; d) PS96/080-1 120 cm cmbsf. Each X-radiograph is 10 cm wide, and white areas are voids in the sediment slabs caused by large gravel grains/pebbles or sample processing. For details of AMS ^{14}C dates, see Table DR2.

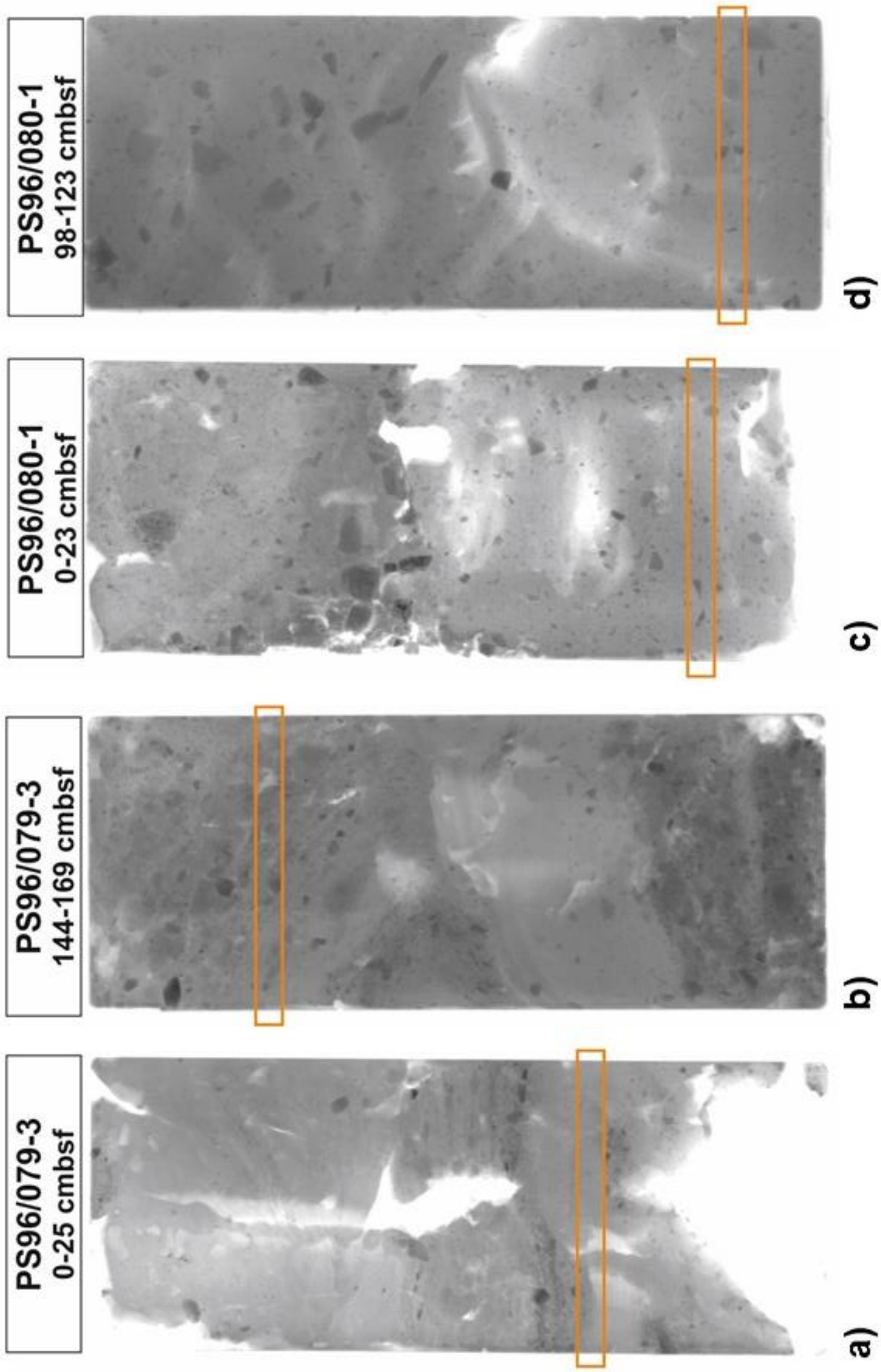
PS96/079-3
0-25 cmbsf
a)
PS96/079-3
144-169 cmbsf
b)
PS96/080-1
0-23 cmbsf
c)
PS96/080-1
98-123 cmbsf
d)

SUPPLEMENTARY REFERENCES

Anderson, J. B., and Andrews, J. T., 1999, Radiocarbon constraints on ice sheet advance and retreat in the Weddell Sea, Antarctica: Geology, v. 27, p. 179-182.

Arndt, J. E., Schenke, H. W., Jakobsson, M., Nitsche, F. O., Buys, G., Goleby, B., Rebesco, M., Bohoyo, F., Hong, J.-K., Black, J., Greku, R., Udintsev, G., Barrios, F., Reynoso-Peralta, W., Taisei, M., and Wigley, R., 2013, The International Bathymetric Chart of the Southern Ocean (IBCSO) Version 1.0 - A new bathymetric compilation covering circum-Antarctic waters: Geophysical Research Letters, v. 40, p. 3111-3117.

Domack, E.W., Jacobson, E.A., Shipp, S., and Anderson, J.B., 1999, Late Pleistocene-Holocene retreat of the west Antarctic ice-sheet system in the Ross sea: Part 2. Sedimentologic and stratigraphic signature: Geological Society of America Bulletin, v. 111, p. 1517-1536.

Heroy, D.C., and Anderson, J.B., 2007, Radiocarbon constraints on Antarctic Peninsula Ice Sheet retreat following the Last Glacial Maximum (LGM): Quaternary Science Reviews, v. 26, p. 3286-3297.

Hillenbrand, C.-D., Larter, R.D., Dowdeswell, J.A., Ehrmann, W., Ó Cofaigh, C., Benetti, S., Graham, A.G.C., and Grobe, H., 2010, The sedimentary legacy of a palaeo-ice stream on the shelf of the southern Bellingshausen Sea: clues to West Antarctic glacial history during the Late Quaternary: Quaternary Science Reviews, v. 29, p. 2741-2763.

Hillenbrand, C.-D., Melles, M., Kuhn, G., and Larter, R. D., 2012, Marine geological constraints for the grounding-line position of the Antarctic Ice Sheet on the southern Weddell Sea shelf at the Last Glacial Maximum: Quaternary Science Reviews, v. 32, p. 25-47.

McKay, R., Browne, G., Carter, L., Cowan, E., Dunbar, G., Krissek, L., Naish, T., Powell, R., Reed, J., Talarico, F., and Wilch, T., 2009, The stratigraphic signature of the late Cenozoic Antarctic Ice Sheets in the Ross Embayment: Geological Society of America Bulletin, v. 121, p. 1537-1561.

McKay, R., Naish, T., Powell, R., Barrett, P., Scherer, R., Talarico, F., Kyle, P., Monien, D., Kuhn. G., Jackolski, C., and Williams, T., 2012, Pleistocene variability of Antarctic Ice Sheet extent in the Ross Embayment: Quaternary Science Reviews, v. 34, p. 93-112.

Miller, H., and Oerter, H. (eds.), 1991, The Expedition ANTARKTIS-VIII of RV “Polarstern” 1989/1990 – Report of Leg ANT-VIII/5: Reports on Polar and Marine Research, v. 86, 155 pp.

Passchier, S., Browne, G., Field, B., Fielding, C.R, Krissek, L.R, Panter, K., Pekar, S.F., and the ANDRILL-SMS Science Team, 2011, Early and middle Miocene Antarctic glacial history from the sedimentary facies distribution in the AND-2A drill hole, Ross Sea, Antarctica: Geological Society of America Bulletin, v. 123, p. 2352-2365.

RAISED Consortium, 2014, A community-based geological reconstruction of Antarctic Ice Sheet deglaciation since the Last Glacial Maximum: Quaternary Science Reviews, v. 100, p. 1-9.

Reimer, P. J., Bard, E., Bayliss, A., Beck, J. W., Blackwell, P. G., Bronk Ramsey, C., Buck, C. E., Cheng, H., Edwards, R. L., Friedrich, M., Grootes, P. M., Guilderson, T. P., Haflidason, H., Hajdas, I., Hatté, C., Heaton, T. J., Hoffmann, D. L., Hogg, A. G., Hughen, K. A., Kaiser, K. F., Kromer, B., Manning, S. W., Niu, M., Reimer, R. W., Richards, D. A., Scott, E. M., Southon, J. R., Staff, R. A., Turney, C. S. M., and van der Plicht, J., 2013, INTCAL13 and MARINE13 radiocarbon age calibration curves, 0–50,000 years cal BP: Radiocarbon, v. 55, no. 4, p. 1869-1887.

Schröder, M. (ed.), 2016, The Expedition PS96 of the Research Vessel POLARSTERN to the southern Weddell Sea in 2015/2016: Reports on Polar and Marine research, v. 700, 143 pp.

Stolldorf, T., Schenke, H.-W., and Anderson, J. B., 2012, LGM ice sheet extent in the Weddell Sea: evidence for diachronous behavior of Antarctic Ice Sheets: Quaternary Science Reviews, v. 48, p. 20-31.

Stuiver, M., and Reimer, P.J., 1993, Extended ^{14}C data base and revised CALIB 3.0 ^{14}C age calibration program: Radiocarbon, v. 35, p. 215-230.

Tripsanas, E., Piper, D.J.W., Jenner, K.A., and Bryant, W.R., 2008, Submarine mass-transport facies: new perspectives on flow processes from cores on the eastern North American margin: Sedimentology, v. 55, p. 97-136.

Wacker, L., Bonani, G., Friedrich, M., Hajdas, I., Kromer, B., Němec, M., Ruff, M., Suter, M., Synal, H. A., and Vockenhuber, C., 2010, MICADAS: Routine and High-Precision Radiocarbon Dating: Radiocarbon, v. 52, no. 2-3, p. 252-262.